CHEMISTRY
A EUROPEAN JOURNAL

DOI: 10.1002/chem.200701265

Understanding Lead Chemistry from Topological Insights: The Transition between Holo- and Hemidirected Structures within the $[Pb(CO)_n]^{2+}$ Model Series

Christophe Gourlaouen, Hélène Gérard, Jean-Philip Piquemal, and Olivier Parisel*[a]

Abstract: In this Contribution, we focus to the currently unknown $[Pb(CO)_n]^{2+}$ model series ($n=1$ to 10), a set of compounds which allows us to investigate in-depth the holo- and hemidirectional character that lead complexes can exhibit. By means of DFT computations performed using either relativistic four-component formalisms coupled to all-electron basis sets for $[Pb(CO)]^{2+}$, $[Pb(OC)]^{2+}$ and $[Pb(CO)_2]^{2+}$, or scalar relativistic pseudopotentials for higher n values, the structure and the energetics of these species are investigated. The results are complemented by Constrained Space Orbital Variations (CSOV) and Electron Localization Function (ELF) comprehensive analyses in order to get better insights into the poorly documented chemical fundamentals of the Pb^{2+} cation. Whereas the discrimination between holo- and hemidirected structures is usually done according to the geometry, we here provide a quantitative indicator grounded on $\langle\rho\rangle_{V(Pb)}$, the mean charge density of the valence monosynaptic $V(Pb)$ ELFic basin associated to the metal cation. Free-enthalpy relying discussions show, moreover, that those gas-phase complexes having $n=7$, 8 or 9 may be experimentally instable and should dissociate into $[Pb(CO)_6]^{2+}$ and a number of CO ligands. According to second-order differences in energy, it is anticipated that the $n=3$ or 6 structures should be the most probable structures in the gas phase. Gathering all data from the present theoretical study allows us to propose some concepts that the versatile structural chemistry of Pb^{2+} complexes could rely on.

Keywords: carbonyl metals · ELF (electron localization function) · intermolecular interactions · lead chemistry · VSEPR theory

Introduction

The Pb^{2+} cation has a $[Xe]4f^{14}5d^{10}6s^26p^0$ electronic configuration and exhibits an especially versatile character with respect to the HSAB (Hard and Soft Acids and Bases) theory[1,2] for which it appears as a borderline acid,[3] able to bind to wide families of ligands[4] within very flexible coordination modes (mono- to decacoordinated).[5,6] The fact that it has been used for centuries in manufacturing or, more recently, as an antidetonant in oils, has resulted in a global lead poisoning unambiguously attested since 1965.[7] Its chemical properties make it possible to bind to a number of biochemically relevant systems, which results in saturnism. Zn^{2+}-binding proteins such as ALAD (AminoLevulinic Acid Dehydratase), or Ca^{2+}-binding proteins such as CaM (calmoduline), are known to be targeted by Pb^{2+} in lead intoxications.[8–11]

The aqueous chemistry of lead has been investigated for many years in order to develop, among others, water or soil clean-up processes, probes, sensors or sequestering agents.[12–18] Recently,[19] a theoretical modelling of the solvation of Pb^{2+} has been reported and has provided a description compatible with the sole experimental data known.[20,21] The gas-phase chemistry of Pb^{2+} is less known although a number of species have been experimentally detected.[6,22–24] However, the spectroscopic and theoretical investigations of gas-phase complexes remain surprisingly rare despite available high-level theoretical data.[25] To the best of our knowledge, studies devoted to such species are limited to: $Pb(H_2O)$, $Pb(HO_2)$, PbOH, PbH_2, PbO, PbO_2 and PbO_3.[26–28] Recently, this series has been extended to $[Pb(H_2O)]^{2+}$ and $[Pb(OH)]^{+}$, both compounds involved in the aqueous, and maybe in the atmospheric chemistry of lead.[3,29] It should be pointed out that, within all these spe-

[a] Dr. C. Gourlaouen, Dr. H. Gérard, Dr. J.-P. Piquemal, Dr. O. Parisel
Laboratoire de Chimie Théorique, CNRS UMR 7616
Université Pierre et Marie Curie–Paris 6
Case courrier 137, 4, place Jussieu
75252 Paris Cedex 05 (France)
Fax: (+33) 144-274-117
E-mail: olivier.parisel@lct.jussieu.fr

cies, only PbH_2 has been spectroscopically characterized by means of its IR spectrum,[30,31] but a few other examples have been unambiguously identified: $[Pb_nCO]$,[24] Pb_2, or Pb_2^- for instance.[32]

One among the possible reasons for this lack of theoretical investigations on leaded complexes is the treatment of relativistic effects. Up to now, it has been possible to treat both problems, correlation and relativity, by using scalar relativistic pseudopotentials coupled to the correlated techniques usually used in quantum chemistry.[4,19,24,26,27,29,32–42] However, the examination of relativistic effects at a four-component level of calculation has been reported at various levels of theory for a few mono-leaded structures:[32] PbO,[35] $PbCl_4$,[35] PbH_4,[35,43] $Pb(CH_3)_3H$,[43] $[Pb(H_2O)]^{2+}$,[29] and $[Pb(OH)]^+$.[29]

Lead complexes exhibit the fundamental characteristic of being either hemi- or holodirected, as depicted in Figure 1, according to the capability of the Pb^{2+} valence lone pair to

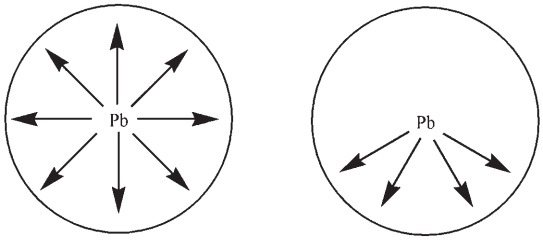

Figure 1. Pb^{2+} complexes can be either holodirected (left) or (right) hemidirected (see ref. [5]).

localize and become spatially directed, or to remain holotropic, thus inducing holodirected structures.[5,16,44] Following our previous investigations on leaded compounds,[19,29,45–46] we will herein investigate this topological transition within the $[Pb(CO)_n]^{2+}$ series. We anticipate that this contribution will stimulate refined theoretical and spectroscopic gas-phase investigations on such complexes. While investigations on the neutral $[Pb_n(CO)]$ species ($n=1$–4)[24] and an unsuccessful attempt to detect the anionic system $[Pb(CO)]^-$[47] have been published, to the best of our knowledge, such $[Pb(CO)_n]^{2+}$ complexes have never been reported, neither experimentally nor theoretically.

The paper is organized as follows. We first present the set of methodologies used and then turn to the structural description of the $[Pb(CO)_n]^{2+}$ compounds. Then, the natural charges, the frequencies of the stretching ν(CO) vibrations and the energetics are investigated within the series. Finally, the mean charge density, volume and population of the ELF (Electron Localization Function) basins V_n(Pb) are reported and discussed.

We must emphasize that such investigations will provide a deeper insight into the hemi- or holocharacter of Pb^{2+} complexes, a feature that isoelectronic cations do not exhibit. A better knowledge, if possible relying on rationalized foundations, on the coordination chemistry of this cation is essential for the design of dedicated cryptants relevant for chelation therapy.

Another reading outline can thus be proposed to the reader. It involves a technical level, namely comparing results based on pseudopotentials to all-electron relativistic computations. Then, comes a more conceptual level, relevant to the underlying laws governing the holo- or hemicharacter that Pb^{2+} complexes can adopt, in order to refine the VSEPR (Valence Shell Electron Pair Repulsion) theory[48–50] or advanced molecular force fields[51] (even polarisable force fields cannot account for the hemi-/holodirected transition, yet, which precludes in-depth modelling of saturnism problems). Finally, applications to the rationalized design of selective ligands could find an interest in the present study.

Methodologies

Computational details: The scalar calculations have been performed using the Gaussian03 package[52] within the Restricted Hartree–Fock (RHF) and B3LYP[53,54] formalisms. This functional, which was successfully used in previous works devoted to Pb^{2+} and other heavy cations,[29,45,55] was chosen as it has proven to provide geometries and energies close to CCSD(T) for species closely related to those investigated here.[26,27,28]

The standard 6-31+G** basis set was used to describe the C and O atoms, whereas scalar relativistic pseudopotentials[56] (PP) were considered for Pb^{2+}. These are either the LANL2DZ/PP by Hay and Wadt[57] coupled to a double-zeta quality basis set described by the (3s3p)/[2s2p] contraction, or the large-core relativistic SDD PPs by Dolg et al.[58] coupled to a (4s4p1d)/[2s2p1d] contraction to describe the valence electrons. We also have investigated the Averaged Relativistic Effective PPs (AREP)[59] known in the EMSL database[60] under the CRENBL ("small-core": valence = 5d,6s,6p) and CRENBS ("large-core": valence = 6s,6p) acronyms. The CRENBS PP considered here is coupled to a valence (3s3p)/[1s1p] basis set whereas the CRENBL uses a (3s3p4d)/[1s1p1d] contraction. The aug-cc-pVmZ small-core PP by Peterson have also been considered for $m=2$ to 5.[61] The valence description is here achieved by means of the following contractions: (8s6p6d)/[4s3p2d], (12 s11p8d1f)/[5s4p3d1f], (14s11p11d2f1g)/[6s6p4d2f1g] and (16s13p12d3f2g1h)/[7s7p5d3f2g1h], respectively. All of them have been supplemented by sets of semi-diffuse orbitals determined as explained in ref. [61]. When using these pseudopotentials, the relevant aug-cc-pVmZ basis sets by Dunning were considered for C and O.[62]

The All-Electron (AE) calculations have been performed using the Faegri's basis set for Pb^{2+}; such a basis set is known to be of at least double-zeta quality.[63]

The four-component calculations have been performed using the DIRAC code[64] which has been recently extended to the DFT formalism.[65,66] The Dirac-Coulomb Hamiltonian[67] (thereafter, DHF/AE: Dirac-HF, DB3LYP/AE: Dirac-B3LYP) has been considered. The uncontracted small component basis sets were generated from the large component

sets according to the kinetic balance condition. Finite size Gaussian nuclei were used and the nuclear exponents were taken from a list of recommended values.[68] All (SS/SS) and (SS/LL) integrals have been retained in the calculations.

Optimizations, vibrational analysis: Full geometry optimizations have been performed. The nature of the stationary points encountered has been characterized by a vibrational analysis performed within the harmonic approximation. No scaling procedure has been applied but a factor of 0.973 can be derived from the comparison of the experimental (2143 cm^{-1}) and computed (2203 cm^{-1}, B3LYP/6-31+G**) ν(CO) stretching vibration in free CO. The unscaled vibrational frequencies computed within the harmonic approximation have been retained to evaluate ΔE_{ZPE}, the Zero-Point-Energy (ZPE) correction, and to estimate free-enthalpies ($T=298$ K, $p=1$ atm).

Interaction energies: The complexation energies used hereafter are defined according to the formation reaction:

$$Pb^{2+} + nCO \rightarrow [Pb(CO)_n]^{2+}$$

$$\Delta_f E(n) = E([Pb(CO)_n]^{2+}) - E(Pb^{2+}) - nE(CO)$$

The Basis Set Superposition Error (BSSE) correction has been determined according to the counterpoise procedure applied to the previous reaction ($n+1$ fragments).[69,70] The binding energy is then defined as:

$$D_0(n) = [\Delta_f E(n) + \Delta E_{BSSE}(n) + \Delta E_{ZPE}(n)]$$

where:

$$\Delta E_{ZPE}(n) = ZPE([Pb(CO)_n]^{2+}) - nZPE(CO)$$

We have also considered the formation free-enthalpies according to:

$$\Delta_f G(n) = G([Pb(CO)_n]^{2+}) - G(Pb^{2+}) - nG(CO)$$

The incremental first-order differences in energy correspond to:

$$\Delta_1 E(n) = E([Pb(CO)_n]^{2+}) - E([Pb(CO)_{n-1}]^{2+}) - E(CO)$$

$$\Delta_1 G(n) = G([Pb(CO)_n]^{2+}) - G([Pb(CO)_{n-1}]^{2+}) - G(CO)$$

Finally, the second-order differences in energy read as:

$$\Delta_2 E(n) = E([Pb(CO)_{n+1}]^{2+}) + E([Pb(CO)_{n-1}]^{2+}) - 2E([Pb(CO)_n]^{2+})$$

This quantity has been widely considered in cluster physical chemistry and has helped to rationalize the concept of magic numbers. It has been applied either to homogenous clusters[71–76] or to heterogeneous clusters such as XC_n^+ for example.[77] It has been extended to encapsulated atoms or ions in clusters such as M@Si_n or M@Ge_n,[78,79] Co@Si_n,[80] or Ti@Si_n.[81] In this contribution, the series under investigation is formally relevant to chemical $[Pb(CO)_n]^{2+}$ entities, but it can also be considered as a set of $[(Pb^{2+})@(CO)_n]$ clusters. $\Delta_2 E(n)$ is a sensitive quantity that reflects the stability of clusters. It can be directly related to experimental relative abundances determined by mass spectrometry.[73,74]

Charge determination and ELF topological analysis: Natural Population Analyses (NPA) have been carried out following the implementation made in Gaussian 03.[52,82] In order to provide a refined analysis, ELF (Electron Localization Function) calculations[83,84] have been performed using the TopMod package.[85,86] The topological analysis of this function and integration over the localization basins have been realized.[87–90] Within the framework of the topological analysis of the ELF function, space is partitioned into basins of attractors, each of them having a chemical meaning. Such basins are classified as:[86] i) core basins surrounding nuclei, and ii) valence basins characterized by their synaptic order.

A core basin, C(X), where X stands for a nucleus, is usually representative of electrons not involved in the chemical bonding, namely non-valence and internal-shell electrons. The valence basins are distinguished according to the number of core basins with which they share a common boundary (synaptic order). A valence basin V(X) is monosynaptic and corresponds to lone-pair or non-bonding regions. A V(X,Y) basin is disynaptic: it connects the core of two nuclei X and Y and, thus, corresponds to a bonding region between X and Y. In principle, the topological analysis of ELF should be restrained to all-electron densities since, without core electrons, there is no core basins and, thus, no way of rigorously define the synaptic order of the valence basins. It has been shown, however, that it is possible to extend the ELF approach to pseudopotentials.[29,91] If using large core pseudopotentials, the number and the location of the valence basins are identical to the all-electron case. Using small-core pseudopotentials provides a semi-external core used to determine the synapticity of well-defined basins for the valence electrons.[92]

In the present contribution, we will only consider V(Pb), the valence monosynaptic basin associated to the valence electrons of Pb^{2+}, and, in practice, to electrons associated to the 6s (valence electrons) and 6p (electron donated by the ligands) orbitals. For a given complex $[Pb(CO)_n]^{2+}$, we will use the following notations: V_n(Pb) is the ELF basin defined previously, N_n(Pb) and ω_n(Pb) are the population and the volume, respectively, associated to this basin. $\langle\rho\rangle_{V_n(Pb)}$ is the corresponding mean charge density:

$$\langle\rho\rangle_{V_n(Pb)} = N_n(Pb)/\omega_n(Pb)$$

CSOV energy decompositions:[93–95] It was found of interest to complement the NPA and ELF analyses by energy decompositions. Among the different existing decomposition schemes,[96–102] we have retained the Constrained Space Or-

bital Variation (CSOV) approach as implemented in our modified version of HONDO95.3.[103,104] The interaction energy ΔE_{AB} between two fragments A (here, CO) and B (here, Pb^{2+}) is then split into different components:

$$\Delta E_{AB} = E_1 + E_2 + \delta E$$

where:

$$E_1 = E_{FC}$$

$$E_2 = E_{pol} + E_{ct} = E_{pol\,A} + E_{pol\,B} + E_{ct\,A\rightarrow B} + E_{ct\,B\rightarrow A}$$

$$\Delta E = \Delta E_{AB} - E_1 - E_2$$

where $E_1(E_{Frozen\,Core})$ includes electrostatic and exchange/Pauli repulsion terms; E_2 is the sum of a charge transfer (E_{ct}) term and of a polarization (E_{pol}) term which can both be split into contributions originating from A and B; δE accounts for some higher-order many-body terms having different physical origins,[105–108] not detailed within the standard CSOV decomposition; they are expected to be small with respect to ΔE_{AB}.

Such an approach has been validated within the framework of DFT,[104,109–112] and has recently been extended to pseudopotential calculations on monohydrate cations of heavy elements.[29,55] With such an energy decomposition, it can a priori be clearly established what is the dominant origin of the complexation energy; this makes then possible to characterize the complex as a covalent (E_2 is the largest component in this case) or as an electrostatic (E_1 is the largest component) species.

In the version of HONDO we have used, there is no handling of h (l=5) spherical harmonics so that the energy decompositions could not be performed using the exact SDD pseudopotential considered. Consequently, we have used for the CSOV decompositions a modified pseudopotential (SDD*) in which the h component has been removed: the resulting variations in ΔE_{AB} are included in δE.

Results

Linear structures: $[Pb(CO)]^{2+}$ versus $[Pb(OC)]^{2+}$

Two coordination modes have been envisioned for the first coordination of CO to the Pb^{2+} cation, either toward the carbon end of the CO ligand ($[Pb(CO)]^{2+}$) or toward its oxygen end ($[Pb(OC)]^{2+}$). This enables us to investigate, respectively, the "soft" side and the "hard" side of the ligand according to the HSAB description.[1]

$[Pb(CO)]^{2+}$: We first investigate coordination by the carbon atom (Table 1). The fully relativistic four-component AE calculations show a weak influence of both relativity and correlation on the geometry, which is found linear in all cases. The relativistic contraction of the Pb–C bond length amounts to 0.037 Å (RHF vs DHF) while correlation (RHF vs B3LYP) decreases that bond by 0.067 Å. The effect of correlation is thus significantly larger than that of relativity. The sum of these bond length reductions amounts to 0.104 Å, a value to be compared to the 0.126 Å decrease deduced from the RHF versus DB3LYP comparison. There is thus a slight synergetic effect (0.022 Å) of correlation and relativity on the Pb–C bond length. Similar conclusions are drawn for the complexation energy as it is increased by $-1.9\,kcal\,mol^{-1}$ by relativity and by $-10.4\,kcal\,mol^{-1}$ by electronic correlation, the sum of which is slightly smaller than the $-13.8\,kcal\,mol^{-1}$ value obtained by the RHF versus DB3LYP comparison. The SDD pseudopotential provides results close to those obtained by means of AE calculations: the difference is only 0.005 Å for the Pb–C bond length. The agreement drops if using LANL2DZ or CRENBS. The discrepancy rises up to more than 0.1 Å using the CRENBL pseudopotential. The LANL2DZ complexation energy is underestimated by $5.6\,kcal\,mol^{-1}$ with respect to the DB3LYP/AE value. The aug-cc-pVmZ-PP results follow, especially for the geometries, those obtained at the SDD level. Concerning the energies, a slightly better agreement to the DB3LYP/AE computations is in fact obtained for $m=4$ or 5 but using such PP's would considerably increase the computational efforts for the higher n $[Pb(CO)_n]^{2+}$ structures (up to $n=10$). We thus have retained the SDD PPs for the remaining of this study.

Table 1. Geometrical parameters and energy data for $[Pb(CO)]^{2+}$. Bold values correspond to reference values.

Basis set	Method	Pb–C [Å]	C=O [Å]	$\Delta_t E(1)$[a]
AE	RHF	2.792	1.097	−19.4
	DHF	2.755	1.096	−21.3
	B3LYP	2.725	1.123	−29.8
	DB3LYP	**2.666**	**1.122**	**−33.2**
SDD	B3LYP	2.661	1.122	−35.4[b]
LANL2DZ	B3LYP	2.623	1.122	−39.2[b]
CRENBL	B3LYP	2.770	1.123	−27.6[b]
CRENBS	B3LYP	2.722	1.122	−34.5[b]
aug-cc-pVDZ-PP	B3LYP	2.697	1.119	−31.8
aug-cc-pVTZ-PP	B3LYP	2.676	1.111	−32.7
aug-cc-pVQZ-PP	B3LYP	2.674	1.109	−32.8
aug-cc-pV5Z-PP	B3LYP	2.673	1.109	−32.8

[a] Energies in $kcal\,mol^{-1}$. [b] The D_0 values amount to: −28.4 (SDD), −30.5 (LANL2DZ), −25.5 (CRENBL) and −27.5 (CRENBS) $kcal\,mol^{-1}$.

$[Pb(OC)]^{2+}$: We now turn to the isomeric $[Pb(OC)]^{2+}$ species (Table 2). In any case, the Pb–O bond is shorter than the Pb–C bond encountered previously (by about 0.16 Å at the B3LYP/SDD level) whereas the C–O bond length is significantly increased.

As observed for $[Pb(CO)]^{2+}$ the effects of relativity and correlation to the geometry are weak. Only considering the coupled contributions induces a contraction of the Pb–O bond length by 0.03 Å and increases the stabilization energy by $3.9\,kcal\,mol^{-1}$.

The closest results to the DB3LYP/AE computations are obtained using the SDD or CRENBS PPs. LANL2DZ un-

Table 2. Geometrical parameters and energy data for $[Pb(OC)]^{2+}$. Bold values correspond to reference values.

Basis set	Method	Pb–O [Å]	C=O [Å]	$\Delta_f E(1)$[a]
AE	RHF	2.501	1.142	−21.1
	DHF	2.499	1.140	−22.3
	B3LYP	2.501	1.165	−22.6
	DB3LYP	**2.467**	**1.164**	**−25.0**
SDD	B3LYP	2.502	1.164	−26.7[b]
LANL2DZ	B3LYP	2.395	1.167	−31.1[b]
CRENBL	B3LYP	2.574	1.162	−21.3[b]
CRENBS	B3LYP	2.531	1.164	−25.8[b]

[a] Energies in kcal mol^{-1}. [b] The D_0 values amount to: −21.3 (SDD), −24.3 (LANL2DZ), −20.0 (CRENBL) and −21.0 (CRENBS) kcal mol^{-1}.

derestimates the Pb–O bond length and the complexation energy whereas the opposite trend is observed for CRENBL. In both cases, the Pb–O bond length differs by about 0.1 Å from the reference DB3LYP/AE value.

Transition structure: Comparison of the complexation energies for $[Pb(CO)]^{2+}$ and $[Pb(OC)]^{2+}$ shows that C coordination is favoured (Tables 1 and 2): at the B3LYP/SDD level of calculations, the former species is stabilized by 8.7 kcal mol^{-1} with respect to the later.

The potential energy curve depicted on Figure 2 illustrates the transition between the C and O coordination.

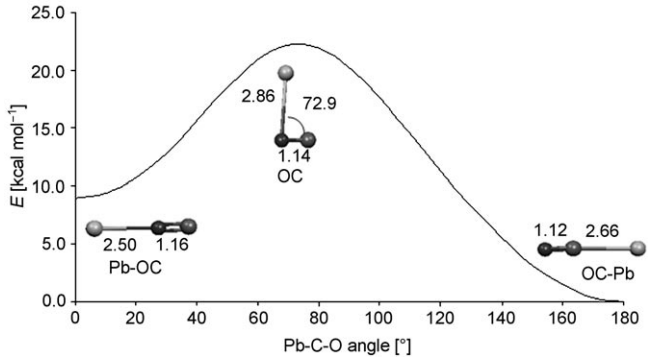

Figure 2. Potential energy curve (B3LYP/SDD) for $[Pb(CO)]^{2+}$ as a function of the Pb-C-O angle. Bond lengths are in Å and angles in degrees.

The transition state exhibits an imaginary vibrational wave number of 249*i* cm^{-1}. It is characterized by a Pb-C-O valence angle amounting to 72.9° and lies about 23 kcal mol^{-1} higher in energy than $[Pb(OC)]^{2+}$ so that CO is hardly bonded (around 3 kcal mol^{-1}) to the cation in the transition state. Interconversion between the O-bonded and the C-bonded isomers should thus take place via decoordination of the carbonyl ligand. The C–O bond length is intermediate to that observed in either $[Pb(CO)]^{2+}$ or $[Pb(OC)]^{2+}$. The Pb–O distance is shorter than the Pb–C one, and amounts to 2.856 Å. It is significantly larger than that observed in $[Pb(OC)]^{2+}$. Such a large increase is in line with the high transition barrier to cross over during the O- to C-coordination process (Figure 2).

Energy and population analysis: The results of the CSOV energy decompositions (B3LYP/SDD*//B3LYP/SDD) are reported in Table 3 for the two isomers. E_1 is slightly positive in both cases. E_2 is negative and ensures the coordination energy. Consequently, both complexes are to be seen as made of two fragments, Pb^{2+} and CO, interacting covalently. The bonding energy is larger (10 kcal mol^{-1}) in the *C*O isomer: this is largely due to a better covalent interaction as E_2 also is 10 kcal mol^{-1} larger in the *C*O complex than in the *O*C structure. As expected from a HSAB description of the bonding, the "softer" C terminus of CO leads to a stronger covalent bonding.

Table 3. CSOV energy decompositions and CSOV components of E_2 for $[Pb(CO)]^{2+}$ and $[Pb(OC)]^{2+}$ (B3LYP/SDD*, kcal mol^{-1}). CT stands for Charge Transfer and TS for the Transition State between the two complexes.

	$[Pb(CO)]^{2+}$	$[Pb(OC)]^{2+}$	TS
ΔE_{AB}	−34.4	−27.4	−13.1
E_1	+5.2	+3.6	12.2
E_2	−40.1	−30.7	−25.6
δE	0.5	−0.3	0.3
cation polarisation	−0.2	−0.3	−0.0
CT: cation to ligand	−4.4	−3.9	−3.9
ligand polarisation	−21.6	−18.2	−12.7
CT: ligand to cation	−13.9	−8.3	−9.0

The consideration of the NPA charges (Table 4) reveals a weak donation from the ligand: it occurs toward the 6p orbitals of the cation and amounts to 0.12 electron for the C coordination and to 0.06 electron for the O coordination. This variation is consistent with the results obtained from the fine analysis of the E_2 term of the CSOV decomposition (Table 3) from which it can be deduced that the leading origin of the stronger coordination of *C*O with respect to *O*C comes from a larger ligand-to-cation charge transfer.

Table 4. Atomic populations (NPA, B3LYP/SDD) for the $[Pb(CO)]^{2+}$ and $[Pb(OC)]^{2+}$ complexes.

	$[Pb(CO)]^{2+}$	$[Pb(OC)]^{2+}$
O	8.24	8.80
C	5.65	5.16
Pb	2.11	2.04

In both cases, the polarisation of the cation and the charge transfer toward the ligand are very small to negligible. The remaining of E_2 is roughly due for 40% to the charge transfer from the ligand to the cation and for 60% to the ligand polarisation in the case of $[Pb(CO)]^{2+}$. For $[Pb(OC)]^{2+}$, these proportions amount to 70:30. The ligand polarization induces an internal charge flow within the carbonyl fragment which takes place from the terminal atom towards that bounded to the metallic cation.

In the transition state, the CSOV energy E_2 reveals results close to, but less pronounced than those observed in $[Pb(OC)]^{2+}$. Especially (Table 3), the variation of the bond-

ing energy between TS and that complex is explained by a less efficient ligand polarisation: as the TS is not linear, and because the Pb-ligand distance is significantly larger, the interactions of Pb^{2+} with the two atoms are not as efficient. E_1 is, however, more destabilizing in TS than in $[Pb(OC)]^{2+}$.

The ELF analysis (Figure 4) shows, for both $[Pb(CO)]^{2+}$ and $[Pb(OC)]^{2+}$, a non-spherical shape of $V_1(Pb)$: it is clearly shifted from the Pb^{2+} nuclei along the Pb–C (or the Pb–O) bond but retains an axial symmetry.

Vibrational analysis: The wave number associated to the CO vibrational stretching amounts to 1992 cm^{-1} in $[Pb(OC)]^{2+}$ and to 2336 cm^{-1} in $[Pb(CO)]^{2+}$ (B3LYP/SDD, Table 5). This last value is larger than that observed for the free carbonyl (computed at 2203 cm^{-1}). Consequently, that complex can be connected to the non-classical series,[113–118] as expected since the 6s orbital does not have the proper symmetry to allow back-donation toward CO. One may object, however, that since a large-core pseudopotential is used, which precludes back-donation from lower 5d or 4f orbitals, this conclusion could be biased. However, Table 1 shows that the geometry of $[Pb(CO)]^{2+}$, and especially the C–O bond length, remain unchanged if considering all-electron calculations for which donation or back-donation processes are fully permitted: this supports the fact that 5d and 4f orbitals are inefficient in increasing back-donation. Since bond lengths are not impacted, the stretching vibration should also remain unaffected in our PP computations.[119–123]

Table 5. NPA charges and ν(CO) frequencies in the $[Pb(CO)_n]^{2+}$ species.

n	Pb[a]	C	O	ν(CO) [cm^{-1}]
1	1.89 (0.12)	0.35	−0.24	2336
2	1.72 (0.30)	0.41	−0.26	2327
3	1.51 (0.52)	0.45	−0.28	2320
4	1.38 (0.65)	0.46	−0.30	$2315_{eq}/2302_{ax}$
5	1.24 (0.79)	0.48	−0.32	$2299_{eq}/2311_{ax}$
6	1.09 (0.92)	0.48	−0.33	2294
7	0.98 (1.03)	0.49	−0.34	2288
8	0.90 (1.12)	0.50	−0.37	2283
9	0.77 (1.25)	0.51	−0.38	2278
10[b]	0.76 (1.25)	0.51 (0.44)	−0.38 (−0.42)	$2277_{prox}/2250_{dist}$

[a] Parenthesized values denote the populations of the 6p orbitals. [b] For that complex, the parenthesized values refer to the distal non-bonding CO ligand.

$D_{\infty h}$ versus C_{2v}: $[Pb(CO)_2]^{2+}$

In the previously investigated monoligated complexes, there cannot be any geometrical restraint imposed to the spatial extension of the valence lone-pair of the Pb^{2+} cation. This external valence orbital is known to become either holotropic (holodirected complex) or directed (hemidirected complex) depending, generally speaking, upon the number and on the nature of the ligating moieties (Figure 1).[5] In this section, we consider $[Pb(CO)_2]^{2+}$ but restrain ourselves to C coordination, which was shown to be the most favoured coordination mode from the investigations reported above on the $[Pb(CO)]^{2+}$ and $[Pb(OC)]^{2+}$ species.

All geometry optimizations have started from C_s structures allowed to relax into higher symmetries, namely C_{2v} or $D_{\infty h}$. Table 6 collects the results: all optimized structures are found C_{2v}. The C-Pb-C angles adhere closely to 90°, a value significantly smaller than that expected from the AX_2E bonding scheme deduced from the electron count and the application of the VSEPR model (120°).[48–50]

Table 6. Geometrical parameters and energetic for $[Pb(CO)_2]^{2+}$. Bold values correspond to reference values.

Basis set	Method	Pb–C[a]	C=O[a] (average)	C-Pb-C [°]	$\Delta_f E(2)$[b]
AE	RHF	2.816	1.098	78.9	−36.3
	DHF	2.768	1.097	82.3	−39.5
	B3LYP	2.741	1.123	82.9	−54.8
	DB3LYP	**2.687**	**1.123**	**87.8**	**−60.5**
SDD	B3LYP	2.711	1.123	86.0	−61.2[b]
LANL2DZ	B3LYP	2.664	1.123	84.4	−66.4[b]
CRENBL	B3LYP	2.794	1.124	85.8	−50.9[b]
CRENBS	B3LYP	2.733	1.123	90.2	−60.9[b]

[a] Bond lengths in Å and energies in kcal mol^{-1}. [b] The D_0 values amount to: −51.6 (SDD), −54.9 (LANL2DZ), −47.4 (CRENBL) and −51.7 (CRENBS) kcal mol^{-1}.

Relativity decreases the Pb–C bond length by 0.05 Å and correlation by a supplementary 0.07 Å. The net contraction amounts to 0.13 Å (RHF vs DB3LYP) showing that, in this case, no synergetic effects appear between relativity and correlation. However, both correlation and relativistic effects appear to play an important role on the exact value of the C-Pb-C angle, increasing its value by nearly 10° between the RHF and DB3LYP geometries. The different pseudopotentials considered perform as described previously: SDD and CRENBS provide results close to the AE relativistic calculations. LANL2DZ generates an acceptable geometry but overestimates the complexation energy whereas using CRENBL results in too long Pb–C bond lengths and, consequently, in a too weak complexation energy.

Comparing the geometry obtained at the B3LYP/SDD level of calculations to that of the monocoordinated complex, we only observe a slight weakening of the coordination to Pb^{2+}. It is characterized by a small decrease of the bonding energy per CO (by 4.8 kcal mol^{-1}), consistent with the lengthening of the Pb–C bond (0.045 Å). Additionally, the two ν(CO) vibrations differ by 1 cm^{-1}, thus revealing no coupling between one an other, and average to 2327 cm^{-1}, a value slightly smaller (by 9 cm^{-1}) than that computed in $[Pb(CO)]^{2+}$.

As seen from the potential energy curve depicted in Figure 3 (B3LYP/SDD), the linear $[Pb(CO)_2]^{2+}$ structure appears as a transition state between two identical C_{2v} species. The associated imaginary vibrational wave number amounts to 31i cm^{-1} and the interconversion barrier to 7.2 kcal mol^{-1}, which is far below the CO bonding energy. Nevertheless, reaching the TS leads to a significant lengthening of the Pb–

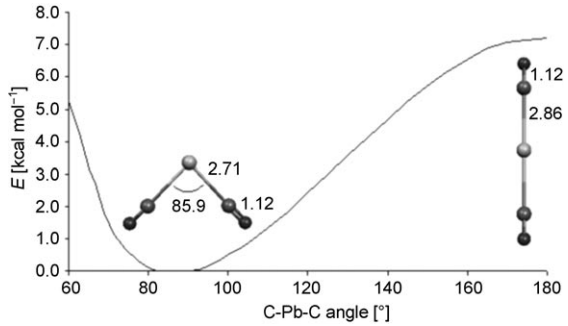

Figure 3. Potential energy curve for $[Pb(CO)_2]^{2+}$ as a function of the C-Pb-C angles. Bond lengths are in Å and angles in degrees.

C distance (0.15 Å), whereas the C–O distance is completely unaffected. This small energy barrier and the large increase of the Pb–C bond length are first evidences of the flexibility of coordination around the Pb^{2+} cation.

Despite the small C-Pb-C angle, the topological analysis of the ELF function supports the AX_2E character of the C_{2v} species. In fact, the hemidirected features of the structure are well evidenced by the representation of V_2(Pb), which exhibits a clear non-spherical character, and a shift of its attractor outside the molecule along the C_2 symmetry axis (Figure 4).

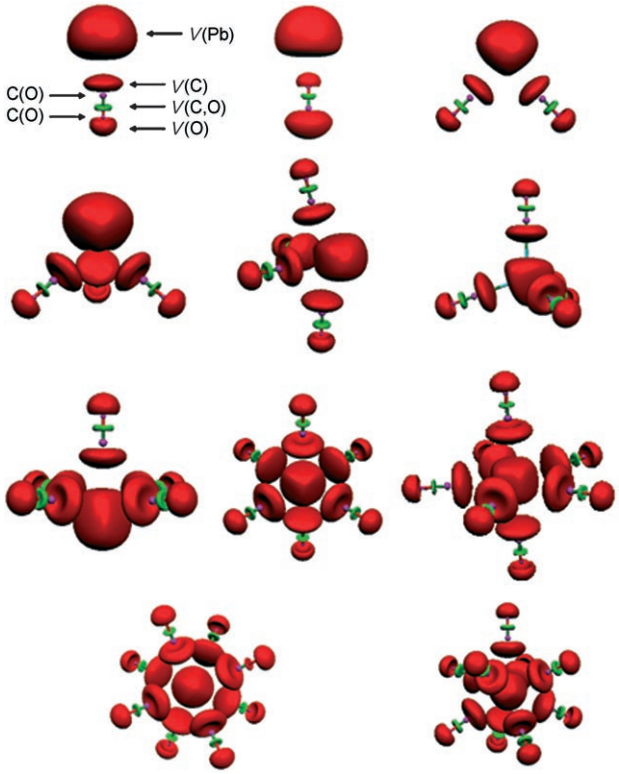

Figure 4. Topology of the ELF function ($\eta = 0.83$) for $[Pb(CO)_n]^{2+}$, $n = 1$ to 9. From top to bottom and from left to right: a) $[Pb(CO)]^{2+}$, $[Pb(OC)]^{2+}$, $[Pb(CO)_2]^{2+}$; b) $[Pb(CO)_3]^{2+}$, $[Pb(CO)_4]^{2+}$ (C_{2v} hemidirected), $[Pb(CO)_4]^{2+}$ (T_d holodirected); c) $[Pb(CO)_5]^{2+}$, $[Pb(CO)_6]^{2+}$, $[Pb(CO)_7]^{2+}$; d) $[Pb(CO)_8]^{2+}$, $[Pb(CO)_9]^{2+}$. Core basins C(C) and C(O) are in purple, valence disynaptic basins V(C,O) in green, and valence monosynaptic basins V(O), V(C) and V(Pb) in red.

From $[Pb(CO)_3]^{2+}$ to $[Pb(CO)_5]^{2+}$

As previous systems and our previous work have shown the reliability of the B3LYP/SDD approach,[19,29,45–46,55] we will from now on restrict ourselves to this framework. The results related to tri- or tetracarbonyl complexes are gathered in Table 7.

Table 7. Geometrical parameters and energetic for $[Pb(CO)_3]^{2+}$ and $[Pb(CO)_4]^{2+}$ (B3LYP/SDD).

Complex	Symmetry	Pb–C[a]	C=O[a]	C-Pb-C[a]	$\Delta_f E(n)$[b]	$\Delta_f G(n)$[b]
$[Pb(CO)_3]^{2+}$	C_{3v}	2.736	1.124	86	−83.0	−58.0
$[Pb(CO)_4]^{2+}$	C_{2v}	2.743/2.897	1.126	86/129/157	−96.9	−63.4
$[Pb(CO)_4]^{2+}$	T_d	2.887	1.125	110	−94.1	−58.7
$[Pb(CO)_4]^{2+}$	D_{4h}	2.917	1.126	90	−90.8	−55.5

[a] Bond lengths in Å and angles in degrees. [b] Energies and free enthalpies in kcal mol^{-1}.

$[Pb(CO)_3]^{2+}$: The tricarbonyl complex appears hemidirected and has a C_{3v} symmetry (Figure 4). Again, the C-Pb-C angle is significantly smaller than the expected value for an AX_3E entity from the VSEPR theory (109°). Similar values are nevertheless encountered in various main group AX_3E structures such as SbF_3 (87.3°),[50] for instance.

$[Pb(CO)_4]^{2+}$: For $n = 4$, the hemidirected (Figure 4) *sawhorse* (or *seesaw*) C_{2v} structure is the lowest in energy. Despite its AX_4E electron count, which should correspond to a monovacant trigonal bipyramid (C_{eq}-Pb-C_{eq} about 120°), it resembles a *cis*-divacant octahedron as demonstrated by the C_{eq}-Pb-C_{eq} and C_{ax}-Pb-C_{ax} valence angles amounting to 86° and 157° respectively. For that complex, the binding carbonyls can be put into two sets. Those in equatorial positions are characterized by a "short" Pb–C bond length of 2.743 Å whereas those in axial positions are associated to a "long" Pb–C bond length of 2.897 Å. The former are associated to ν(CO) close to 2315.5 cm^{-1} and the latter to 2302.7 cm^{-1}. This can be compared to the three ν(CO) vibrations in $[Pb(CO)_3]^{2+}$, which differ by less than 1.5 cm^{-1} and average to 2320 cm^{-1}. In addition to the case of the dicarbonyl complexes, a significant decrease of ν(CO) with the coordination number is highlighted, although remaining much higher than in free CO. This will be discussed further for the whole series of polycarbonyl complexes, but let us also point out that it is to be related to a small but also systematic increase of the Pb–C distances.

We have investigated a tetracarbonyl structure having an holotropic distribution of the ligands, namely an holodirected structure which would formally be consistent with an AX_4 VSEPR description. The resulting T_d structure is slight-

ly destabilized with respect to the previous C_{2v} hemidirected structure. The energetic difference amounts to 2.8 kcal mol^{-1} and rises to 4.7 kcal mol^{-1} for the free enthalpy. In that tetrahedral complex, all Pb–C bond lengths are identical at 2.887 Å, close to the "long" distances observed in the C_{2v} isomer. Indeed, this structure is not an energy minimum: the vibrational analysis reveals three degenerated imaginary frequencies (T_2 symmetry) corresponding to the distortions of the Pb-C-C-C dihedral angles to recover the *cis*-divacant octahedron. Such a small energy barrier associated to a third-order extremum is a clue for the flexibility of these polycarbonyl complexes. The same remarks apply to the planar D_{4h} structure, still higher in energy, and still a high-order saddle-point. It costs 6.1 kcal mol^{-1} ($\Delta_f E(4)$) and 7.9 kcal mol^{-1} ($\Delta_f G(4)$) to reach this transition structure from the lowest C_{2v} geometry. These values compare favourably with the 8–12 kcal mol^{-1} estimates for converting a hemidirected to a constrained holodirected structure in the absence of strong interactions between the ligands.[5] It should however be kept in mind that the estimates reported in reference [5] have been obtained by means of uncorrelated Hartree–Fock calculations relying on the LANL2DZ PP, a procedure that has been shown insufficient to quantitatively describe heavy metal complexes.[19,29,45–46,55]

$[Pb(CO)_5]^{2+}$: The pentacarbonyl complex exhibits a C_{4v} symmetry and a structure close to an octahedron having lost one axial ligand, in line with an AX_5E structure (a slightly distorted square-based pyramid as the metal cation is not in the plane defined by the four carbon atoms). V_5(Pb) is directional: a slight deformation towards the missing ligand is observed (Figure 4). The axial ligand, corresponding to the short Pb–C distance, is associated to ν(CO) = 2311 cm^{-1}, while the vibration frequencies average to 2299 cm^{-1} for the four basal carbonyl ligands (they differ by less than 1.5 cm^{-1}).

The holodirected D_{3h} structure (which is a trigonal bipyramidal more in line with a formally AX_5 electron count) is found 1.5 kcal mol^{-1} ($\Delta_f E$) and 3.5 kcal mol^{-1} ($\Delta_f G$) higher in energy than the previous hemidirected structure. The axial Pb–C bond lengths amount to 2.917 Å, and the equatorial ones to 2.934 Å. It exhibits two imaginary frequencies at 11.5*i* cm^{-1}.

From $[Pb(CO)_6]^{2+}$ to $[Pb(CO)_{10}]^{2+}$

For *n* rising from 1 to 5, the external valence lone pair of Pb^{2+} remains shifted from the nucleus position and the complexes are hemidirected. Further insight into the flexibility of these species could be obtained from ab initio molecular dynamics simulations.[19] These are under investigations and will be published in due time.

It can be anticipated that increasing the number of carbonyl ligands will induce constraints due to steric hindrance. One way for the resulting complexes to accommodate such steric effects would be to switch into holodirected structures in which the lone pair recovers a holotropic character. The structures and energetics have been collected in Table 8.

$[Pb(CO)_6]^{2+}$: The lowest-energy hexacarbonyl complex exhibits an octahedral structure (formally: AX_6) with six equal Pb–C distances (2.961 Å). Such an arrangement is not in line with the previous structures, as one would have expect-

Table 8. Geometrical parameters and energetic for $[Pb(CO)_n]^{2+}$ (B3LYP/SDD).

Complex[a]	Pb–C[b]	C=O[b]	C-Pb-C[b]	Group	$\Delta_f E(n)$[c]	$\Delta_1 E(n)$[c]	$\Delta_f G$[c]	$\Delta_1 G(n)$[c]
$[Pb(CO)]^{2+}$	2.661	1.122	–	$C_{\infty v}$	−35.4	−35.4	−28.4	−28.4
$[Pb(CO)_2]^{2+}$	2.711	1.123	86	C_{2v}	−61.2	−25.8	−45.7	−17.3
$[Pb(CO)_3]^{2+}$	2.736	1.124	86	C_{3v}	−83.0	−21.7	−58.0	−12.3
$[Pb(CO)_4]^{2+}$	$2.743_{eq}/2.897_{ax}$	1.126	86/129/157	C_{2v}	−96.9	−14.0	−63.4	−5.4
$[Pb(CO)_5]^{2+}$	$2.745_{eq}/2.925_{ax}$	1.125	80/88	C_{4v}	−109.3	−12.4	−67.9	−4.5
$[Pb(CO)_6]^{2+}$	2.961	1.127	90	O_h	−119.8	−10.5	−72.2	−4.3
$[Pb(CO)_7]^{2+}$	$3.017_{eq}/2.969_{ax}$	1.128	72/90	D_{5h}	−127.6	−7.8	−73.1	−0.9
$[Pb(CO)_8]^{2+}$	3.037	1.128	73/77	C_{4v}	−135.1	−7.5	−69.0	+4.1
$[Pb(CO)_9]^{2+}$	$3.067_{eq}/3.133_{ax}$	1.128	70(4)/118(2)/ 135(2)[d]	C_{4v}	−139.9	−4.8	−64.8	+4.2
$[Pb(CO)_{10}]^{2+}$	3.069/3.172/ 4.57[d]	1.128	55(4)/110(4)/ 180(1)[e]	C_{4v}	−142.9	−3.0	−59.8	+2.9

[a] The most stable structure is retained. [b] Bond lengths in Å and angles in degrees. [c] Energies in kcal mol^{-1}. [d] These values refer to the different C_{ax}-Pb-C angles, and to their occurrence. [e] These values refer to the different Cd-Pb-C angles, and to their occurrence.

ed a D_{5h} (AX_6E) monovacant pentagonal-bipyramidal geometry according to the standard VSEPR rules.[48–50,124] However, it has been suggested that "in AX_6E (X = Cl, Br, I) molecules with the O_h geometry the ligands X are sufficiently closely packed around the central atom A so as to leave no space in the valence shell for the lone pair E, which remains part of the core".[124–129] Such octahedral structures are known for example, for $[SnX_6]^{4-}$, $[SbX_6]^{3-}$, $[BiX_6]^{3-}$, $[SeX_6]^{2-}$, or $[TeX_6]^{2-}$ (X = Cl, Br or I), in which the central metallic ion is isoelectronic to Pb^{2+} (ns^2 np^0 valence electronic configuration: n = 4, 5 or 6).[50,124,130–133] The previously-involved cations, namely Sb^{3+}, Bi^{3+}, Se^{4+}, and Te^{4+} are not known, however, and to the best and most knowledge acquired by the authors from the literature, to be the subject of any holo- or hemidirectional dichotomy: these cations' lone pairs have not been reported to have any stereochemical role, at least yet. For the Sn^{2+} cation, things may be subtler and should deserve deeper attention as the interpretation of some crystallographic data remains somehow unclear, as well as for Bi^{3+} engaged in the solid phase.[134,135] Although the cation Pb^{3+} is not isoelectronic with the previous one, we can also notice that the $[PbCl_6]^{3-}$

complex is octahedral.[136] In the currently investigated $[Pb(CO)_6]^{2+}$ structure, the six ν(CO) values differ by less than 2.2 cm^{-1} and average to 2294 cm^{-1}. It is worth noting that, in this highly symmetric structure, no significant coupling of the ν(CO) mode appears.

$[Pb(CO)_n]^{2+}$, $n=7$–8: The heptacoordinated species (formally AX_7E) is a D_{5h} pentagonal bipyramid (thus most consistent with AX_7 complexes) having, this time, axial Pb–C bond lengths (2.969 Å) shorter than the equatorial ones (3.017 Å). The seven ν(CO) vibrations fall within 7.5 cm^{-1} and average to 2288 cm^{-1}.

In the square antiprism (holodirected, C_{4v}) octacoordinated complex, all carbonyl groups are equivalent and the Pb–C bond length (3.037 Å) is slightly longer than those observed in $[Pb(CO)_7]^{2+}$: the values for ν(CO) are within 5 cm^{-1} and average to 2281 cm^{-1}.

The nonacarbonyl complex (Figure 5, left) is holodirected and has a C_{4v} symmetry. The Pb–C bond lengths are within 3.067 and 3.133 Å, still larger than in the lower n complexes, for which a monotonous increase of the bond length was observed with respect to n. The ν(CO) vibrations differ by less than 10 cm^{-1} and average to 2278 cm^{-1} (Table 5).

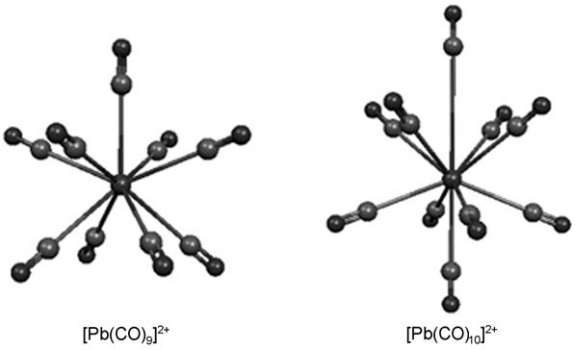

Figure 5. The structure of $[Pb(CO)_9]^{2+}$ and $[Pb(CO)_{10}]^{2+}$.

$[Pb(CO)_{10}]^{2+}$: All attempts to optimize a decacarbonyl structure have failed. Usually, the structure obtained with ten ligands exhibits a long apical Pb–C bond lengths of about 4.57 Å (Figure 5, right): the supplementary carbonyl ligand thus cannot be considered as bounded anymore. Moreover, the C-Pb-C valence angles involving the proximal axial carbonyl and the "equatorial" ones amount to 109.9° whereas those involving the supplementary distal carbonyl decrease to about 55° (Table 8). For such an optimized structure, the 10 ν(CO) frequencies split into a set of nine values closely related to the nine vibrations observed in $[Pb(CO)_9]^{2+}$ which average at 2277 cm^{-1}, and a single value at 2250 cm^{-1} corresponding to the distal ligand. This latter value is still closer to the ν(CO) vibration observed for free CO (computationally obtained at 2203 cm^{-1}). This provides an other hint that this structure should be better described as a $[Pb(CO)_9]^{2+}$ entity weakly interacting with a single CO. Inspection of NPA charges (Table 5) provides an other evidence that there is one non-bonding ligand in the $[Pb(CO)_{10}]^{2+}$ species: there is no variation of the natural charge hold by the metal cation going from $n=9$ to 10 and, thus, no supplementary charge transfer toward the 6p orbitals. Moreover, the distal ligand (Pb–C 4.57 Å) is almost non-polarized, the C–O bond length (1.131 Å) and the CO stretching wave number (2250 cm^{-1}) farther indicate that it is a quasi free ligand. The remaining differences with respect to a purely free carbonyl very certainly come from a residual influence of the metallic cation and from the ligand field induced by the other CO entities.

Discussion

Charge, frequency and energetic considerations

Linear behaviours with n: Additional qualitative insight into the complexation properties of Pb^{2+} can be found in Table 5 with collects the NPA charges for the series of complexes ($n=1$ to 10). Interestingly, the partial charge on Pb^{2+} decreases almost linearly with respect to the number of CO ligands (Figure 6): the charge transfer per CO unit is almost constant from $n=1$ to 9, the exception for $n=10$ having been explained above.

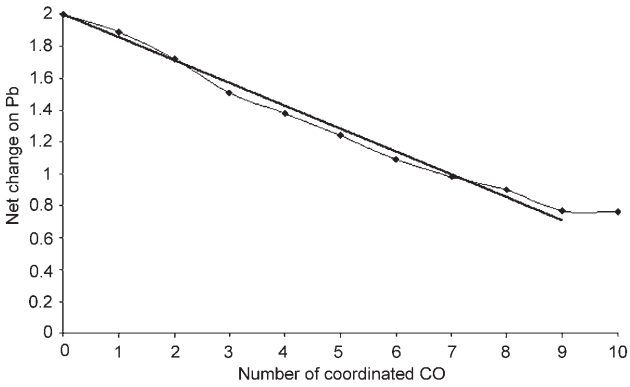

Figure 6. Variations of the NPA charges at the Pb cation with respect to the number of CO ligands in $[Pb(CO)_n]^{2+}$. The linear regression provides: $q(Pb) = -0.1435n + 2$ with a regression coefficient: $R^2 = 0.989$.

This charge transfer mostly takes place from the carbon atoms toward the 6p orbital of the metal cation. It is thus coupled to an increasing polarisation of the ligands: the NPA charges on the carbon atoms increases with n faster than those on the oxygen atoms, thus increasing altogether the charge difference between the two atoms of the carbonyl ligands.

More insights on this ligand polarisation can be gained by examining the hemidirected $[Pb(CO)_4]^{2+}$ and $[Pb(CO)_5]^{2+}$ structures for which the ligands can be put into two sets, distal or proximal, according to the Pb–C bond length. The net charge on the distal carbonyl ligands (+0.17) is slightly larger than that of the proximal ones (+0.14) whereas the

charge difference between C and O in CO remains almost unchanged between the two sets of ligands: 0.76 for the proximal CO, and 0.77 for the distal CO. The polarization of the CO ligand thus does not seem to be related to the Pb–C bond lengths nor to the presence, or not, of a ligand in *trans* position.

Additionally to the charge transfer, the Pb–C bond length increases linearly with n whereas the stretching CO vibration decreases with increasing n. This results in a linear correlation between NPA charges held by Pb^{2+} and vibrational frequencies as reported in Figure 7 for the $[Pb(CO_n)]^{2+}$ series. A clear linear correlation appears, as would have been obtained between ν(CO) and the coordination number.

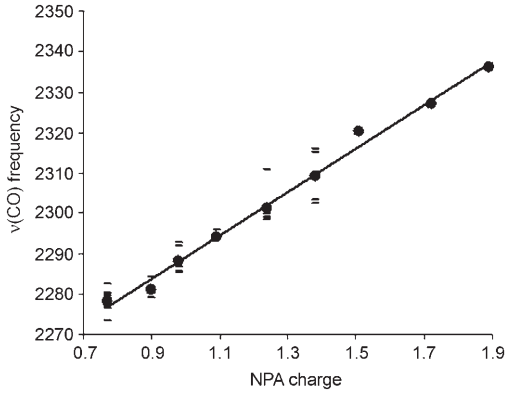

Figure 7. ν(CO) frequencies in cm^{-1} in $[Pb(CO)_n]^{2+}$ as a function of the NPA charge of Pb^{2+}. The frequencies are indicated as dashes. The dots correspond to the average over all ν(CO) for each structure. The linear regression provides: $\nu(CO) = 53.799q(Pb) + 2235.3$ with a regression coefficient $R^2 = 0.993$.

Relative stabilities: Whereas charge transfer, bond lengths and ν(CO) altogether exhibit a number of features consistent with the incremental coordination of CO ligands, the energetic features are not in line with these observations. Up to $n = 5$, attaching CO ligand remains favoured (Figure 8). Even binding the sixth ligand favours the complexation energy by 10.5 kcal mol^{-1}. From $n = 6$, the complexation energies and free enthalpies have different behaviours. $\Delta_f E(n)$ decreases from 7 to 9 whereas $\Delta_f G(n)$ is quasi stable for $n = 7$ and re-increases for $n = 8$ and 9. This is a clear signature of the influence of entropy on the stability of theses complexes. At low temperature, all complexes are expected to be stable from these data. At room temperature ($T = 298$ K at which the G values have been evaluated), or higher, as the entropic term increases, those complexes having $n > 7$ become unstable with respect to those of lower n, and the existence of the heptacarbonyl complex is uncertain and needs further investigations. However, octa- and nonacarbonyl complexes are expected to dissociate into at least $[Pb(CO)_7]^{2+}$ and a number of CO moieties.

Additional conclusions shall be obtained from the second-order difference in energy $\Delta_2 E(n)$.[73,74] Whereas the great

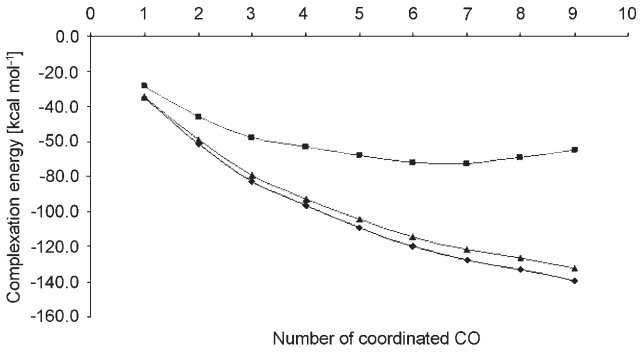

Figure 8. Variations of: $\Delta_f G(n)$ (■); $\Delta_f E(n) + \Delta E_{ZPE}(n)$ (▲); $\Delta_f E(n)$ (◆).

stability of the $n = 6$ structure is in line with the previous observations (Figure 9), it predicts that the $n = 3$ structure should also be observed in gas-phase.

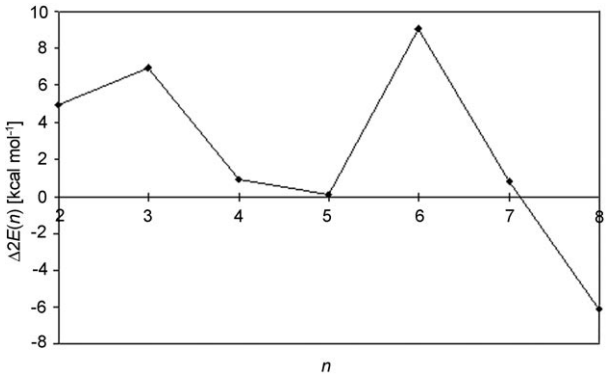

Figure 9. Second-order difference in energy $\Delta_2 E(n)$ in kcal mol^{-1}.

The holo/hemi transition quantified—Consequences

Localisation of the ELF attractors: As mentioned above, in hemidirected arrangements, a single ELF attractor is located *trans* to the proximal ligands (see, for instance, Figure 10). For $n = 4$, it is on the symmetry axis and coplanar with the two proximal CO ligands. For $n = 5$, it is located *trans* to the proximal CO ligands and is collinear to the associated O-C-

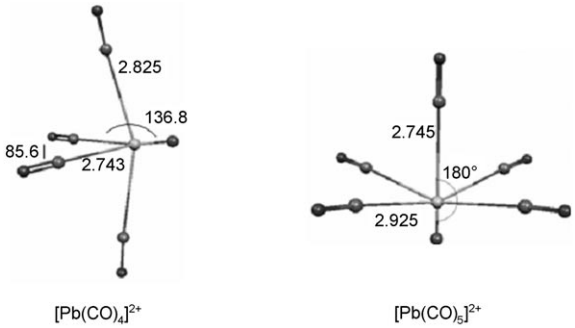

Figure 10. Location of the ELF attractors in $[Pb(CO)_4]^{2+}$ and $[Pb(CO)_5]^{2+}$. Angles in degrees and bond lengths in Å.

Pb direction. For these two complexes, the lone pair thus appears directional and the corresponding V_n(Pb) basin is associated to a well-defined single attractor.

Things are different for $[Pb(CO)_7]^{2+}$ in its pentagonal bipyramidal structure. In that case, the holotropic orientation of the ligands does not favour any privileged direction for the lone pair to expand. We note that the set of carbon atoms (or the set of oxygen atoms) makes a decahedron centred on the metal cation. The directions defined by Pb^{2+} and the centres of the faces of such decahedrons thus constitute regions of minimal electronic density toward which one expects the lone pair to expand the most easily. This is exactly what is observed when investigating the ELF attractors (Figure 11): V_7(Pb) is not associated to a single attractor, but to 10 attractors exhibiting an holotropic distribution around the metal cation. The same observations can be drawn for the holodirected $n=6$ (an octahedral structure thus having eight faces), for which the bifurcation diagrams[88] reveals eight attractors.

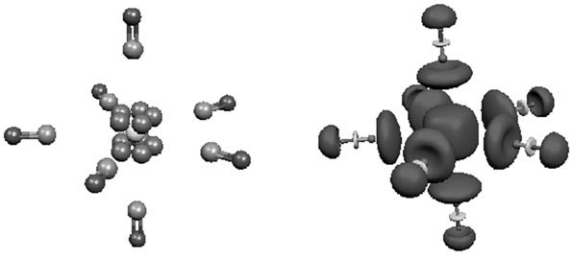

Figure 11. Location of the ELF attractors (left) corresponding to the ELF basin (right, $\eta=0.85$) of the lone pair for $[Pb(CO)_7]^{2+}$.

However, the octacarbonyl complex (a square-antiprism structure having 10 faces) only possesses two attractors on the C_4 axis. V_9(Pb) is associated to four attractors only: increasing the number of ligands increases the mean electronic density around the metal cation and decreases the number of privileged directions the lone pair can distort toward. In all these cases ($n=6$ to 9), V_n(Pb) do not involve any contribution from the CO ligands: it has thus become chemically inert. At the opposite, for $n=1$ to 5 structures, slight contributions from the C atoms are observed.

Linear variations of $\langle\rho\rangle_{V_n(Pb)}$ and ω_n(Pb) up to $n=6$: Apart from geometrical differences, increasing the coordination induces an increase of N_n(Pb) as seen from Table 9. This is fully in line with the charge decrease at Pb revealed by the NPA analysis. Concomitantly, a decrease of ω_n(Pb) appears. Increasing the number of ligands around the metallic cation thus compresses the metallic valence pair as the volume ω_n(Pb) decreases, despite the simultaneous increase of the Pb–C bond lengths. Consequently, the mean charge density $\langle\rho\rangle_{V_n(Pb)}$ increases drastically: it is almost tripled going from $n=0$ to 9. This can be connected to the smaller and smaller gain in the coordination energy when increasing the number of ligands as the energetic cost of such a compression of the valence pair (an increased electronic density increases the Coulomb repulsion between the two electrons) counter-balances the gain recovered from the coordination of supplementary ligands. The result of this balance appears on Figure 12: $\langle\rho\rangle_{V_n(Pb)}$ increases roughly linearly with n up to 6.

Table 9. Volume ω_n(Pb), population N_n(Pb) and mean charge density $\langle\rho\rangle_{V_n(Pb)}$ of the V_n(Pb) ELF basins in $[Pb(CO)_n]^{2+}$.

n	ω_n(Pb) [au^3]	N_n(Pb) [e$^-$]	$\langle\rho\rangle_{V_n(Pb)}$ [$10^3\times$e$^-$ au^{-3}]
0	362.0	1.99	5.50
1	291.0	2.15	7.39
2	264.0	2.26	8.56
3	240.0	2.34	9.75
4	221.0	2.36	10.68
5	199.0	2.42	12.16
6	170.3	2.45	14.39
7	167.0	2.46	14.73
8	164.3	2.44	14.85
9	163.0	2.44	14.97

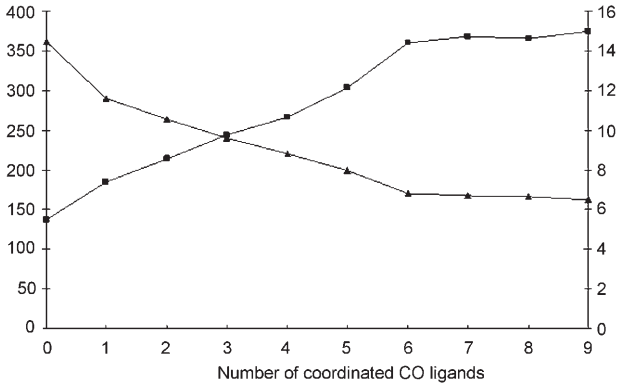

Figure 12. Volume ω_n(Pb) in au^3 (left axis, ▲) and mean charge density $\langle\rho\rangle_{V_n(Pb)}$ in 10^{-3} e$^-$ au^{-3} (right axis, ■) of the V_n(Pb) ELF basins in $[Pb(CO)_n]^{2+}$.

Breaking $\langle\rho\rangle_{V_n(Pb)}$ and ω_n(Pb) at $n=6$: A topological transition toward saturation. From $n=6$, $\langle\rho\rangle_{V_n(Pb)}$ becomes rather constant, reaching a limit value of about 15.0×10^{-3} e$^-$ au^{-3}. Very interestingly, the transition between the linear and the constant behaviour of both ω_n(Pb) and $\langle\rho\rangle_{V_n(Pb)}$ occurs at this same $n=6$ value, which, as seen previously, corresponds to the transition from hemidirected to holodirected structures.

Toward a semi-quantitative model of bonding in Pb^{2+} complexes? In the current $[Pb(CO)_n]^{2+}$ series, the $n=6$ value corresponds to the transition between hemi- (low n values) and holodirected (high n values). It also corresponds to the turning point from which the strict application of the textbook VSEPR rules seems to fail and has to be modified:[50,124–127] for low n values, the complexes follow the rule and adopt (more or less distorted) AX_nE structures, whereas for higher n, structures corresponding to AX_n electron

counts are observed. This alternative electron count seems appropriate as the valence lone-pair has lost its stereochemical activity and can be proposed to act as if merging the core. The existence of saturation plateaus for both $\omega_n(Pb)$ and $\langle\rho\rangle_{V_n(Pb)}$ constitutes a novel feature in the Pb^{2+} chemistry and might provide a clue on how the cation decides its coordination number. If we made the a priori reasonable hypothesis that the limiting value of $\langle\rho\rangle_{V_n(Pb)}$ does not depend on the ligands whereas the amount of donation toward the metal does, it can then be proposed that, in the limit where ligand–ligand repulsions do not play the leading role:

- Pb^{2+} can accommodate up to a large number of weakly donating neutral ligands. As the coordination is high, the resulting structures are likely to be holodirected.
- At the opposite, when Pb^{2+} coordinates to strong donating ligands, the limiting value of the mean charge density $\langle\rho\rangle_{V_n(Pb)}$ will be reached for low coordination numbers. It is then unlikely that the number of ligands can be increased, and the resulting species will most probably adopt a hemidirected structure. In those cases, $V_n(Pb)$ will point toward the vacancy left by the missing ligands.

From this viewpoint, *C*O should be considered as a relatively weak σ-donor, and stronger donating ligands should be obtained using anionic species. These points, and especially the constancy of the limiting value with respect to the ligands and the n value corresponding to the hemi- towards holodirected structures, are under investigations and will be published in due time. However, we can already notice that such conclusions are in line with some empirically known factors favouring hemidirected or holodirected structures (*cf.* Table 6 of ref. [5]).

Conclusion

The analysis of the complexation energies reveals the stability, with respect to isolated Pb^{2+} and CO, of the $[Pb(CO)_n]^{2+}$ species up to n = 9, but that relying on the free enthalpies indicates a maximum of thermodynamic stability for $n=7$ at $T=298$ K. Second-order difference in energy reveals, however, a special stability for the $n=3$ and 6 structures. Experimental investigations should be of interest to determine whether the $n=8$ and 9 complexes exist in the gas phase or whether they dissociate into CO and $[Pb(CO)_7]^{2+}$. Even for $n=7$, the complex require further investigation to confirm its existence. Our calculations show that $[Pb(CO)_{10}]^{2+}$ should in fact be considered as CO weakly interacting with $[Pb(CO)_9]^{2+}$.

In all structures, the Pb–C bond lengths are rather high, more than 2.6 Å, a significantly increased value when compared to transition metal carbonyl complexes.[113] Such large distances allow diminishing the ligand–ligand repulsion and reaching high coordination numbers.

For $n<6$, all structures follow the VSEPR rules and can be described as AX_nE entities, where E is the valence lone pair of the cation. These complexes are hemidirected and the associated $V_n(Pb)$ basins exhibit a clear distortion: they point outside the complexes and occupy void sites. The transition toward a holodirected structure occurs at $n=6$. From this value, the complexes have to be described as AX_n entities as the $6s^2$ lone pair has become stereochemically inert and has merged the VSEPR core. The associated ELF $V_n(Pb)$ basins exhibit holotropic shapes.

This transition at $n=6$ has been quantified by the mean charge density $\langle\rho\rangle_{V_n(Pb)}$ associated to $V_n(Pb)$. From $n=0$, this value increases regularly with n: $V_n(Pb)$ appear being compressed by the ligands. $\langle\rho\rangle_{V_n(Pb)}$ reaches a limiting plateau starting at $n=6$ from which $V_n(Pb)$ cannot be compressed farther, thus loosing any role in determining the subsequent allowed coordination numbers which become governed by ligand–ligand repulsions only.

Acknowledgements

The relativistic four-component calculations have been performed at the CRIHAN regional supercomputing centre (F. 76800 Saint-Etienne-du-Rouvray, France) which is greatly acknowledged for its facilities. The authors are indebted to Dr. T. Saue (ICS, CNRS UMR 7177, Université Louis Pasteur, F. 67000 Strasbourg, France) for his help in using the DIRAC code. Most pseudopotential computations have been performed on the national IDRIS (F. 91403 Orsay, France) and CINES (F. 34097 Montpellier, France) supercomputing centres. The ELF computations have been run at the local CCRE centre at Université Pierre et Marie Curie, Paris 6 (F. 75252 Paris CEDEX 05, France). The authors wish to thank Prof. B. Silvi and Dr. A. Savin, at the Laboratoire de Chimie Théorique (LCT, CNRS UMR 7616, Université Pierre et Marie Curie, Paris 6, F. 75252 Paris CEDEX 05, France), for helpful and stimulating discussions.

[1] R. G. Pearson, *J. Am. Chem. Soc.* **1963**, *85*, 3533.
[2] R. G. Pearson, *Inorg. Chem.* **1988**, *27*, 734.
[3] An experimental illustration of this versatile character comes, for example, from the solubility of PbX_2 halides in water: both PbF_2 (F^- as hard HSAB basis) and PbI_2 (I^- as soft HSAB basis) are poorly soluble in water, see: F. A. Cotton, G. Wilkinson, *Advanced Inorganic Chemistry*, 5th ed., Wiley Interscience, New York, **1988**.
[4] For example: M. Kaupp, P. von Ragué Schleyer, *J. Am. Chem. Soc.* **1993**, *115*, 1061.
[5] L. Shimoni-Livny, J. P. Glusker, C. W. Bock, *Inorg. Chem.* **1998**, *37*, 1853.
[6] L. Puskar, P. E. Barran, B. J. Duncombe, D. Chapman, A. J. Stace, *J. Phys. Chem. A* **2005**, *109*, 273.
[7] C. C. Patterson, *Arch. Environ. Health* **1965**, *11*, 344.
[8] S. J. Lippard, J. M. Berg, *Principles of Bioinorganic Chemistry*, University Science Books, Sausalito (CA, USA), **1994**.
[9] *Collective Handbook of Metalloproteins, Vol. III* (Eds.: A. Messerschmidt, R. Huber, K. Wieghardt, T. Poulos), Wiley, New York, **2004**.
[10] F.-X. Reichl, *Taschenatlas der Toxikologie*, Thieme, Stuttgart, **2002**.
[11] J. Koolman, K.-H. Röhm, *Taschenatlas der Biochemie*, Thieme, Stuttgart, **2003**.
[12] R. Métivier, I. Leray, B. Valeur, *Chem. Commun.* **2003**, 996.
[13] R. Métivier, I. Leray, B. Valeur, *Chem. Eur. J.* **2004**, *10*, 4480.
[14] J. Y. Kwon, Y. J. Jang, Y. J. Lee, K. M. Kim, M. S. Seo, W. Nam, J. Yoon, *J. Am. Chem. Soc.* **2005**, *127*, 10107.
[15] For a recent example, see: A. Pellissier, Y. Bretonnière, N. Chatterton, J. Pécaut, P. Delangle, M. Mazzanti, *Inorg. Chem.* **2007**, *46*, 3714.

[16] E. S. Claudio, M. A. Ter Horst, C. E. Forde, C. L. Stern, M. K. Zart, H. A. Godwin, *Inorg. Chem.* **2000**, *39*, 1391.
[17] C. Platas-Iglesias, D. Esteban-Gomez, T. Enriquez-Pérez, F. Avecilla, A. De Blas, T. Rodriguez-Blas, *Inorg. Chem.* **2005**, *44*, 2224.
[18] D. Esteban-Gomez, R. Ferreiros, S. Fernandez-Martinez, F. Avecilla, C. Platas-Iglesias, A. De Blas, T. Rodiguez-Blas, *Inorg. Chem.* **2005**, *44*, 5428.
[19] C. Gourlaouen, H. Gérard, O. Parisel, *Chem. Eur. J.* **2006**, *12*, 5024.
[20] T. J. Swift, G. Sayre, *J. Chem. Phys.* **1966**, *44*, 3567.
[21] H. Ohtaki, T. Radnai, *Chem. Rev.* **1993**, *93*, 1157.
[22] G. Akibo-Betts, P. E. Barran, L. Puskar, B. Duncombe, H. Cox, A. J. Stace, *J. Am. Chem. Soc.* **2002**, *124*, 9257.
[23] T. Shi, G. Orlova, J. Guo, D. K. Bohme, A. C. Hopkinson, K. W. M. Siu, *J. Am. Chem. Soc.* **2004**, *126*, 7975.
[24] L. Jiang, Q. Xu, *J. Chem. Phys.* **2005**, *122*, 034505.
[25] For other references on compounds awaiting an experimental characterization, despite being well characterized at the theoretical level, see, for instance: a) O. Parisel, M. Hanus, Y. Ellinger, *J. Phys. Chem.* **1996**, *100*, 2926; b) O. Parisel, M. Hanus, Y. Ellinger, *J. Chem. Phys.* **1996**, *104*, 1979; c) O. Parisel, M. Hanus, Y. Ellinger, *Chem. Phys.* **1996**, *212*, 331; d) O. Parisel, M. Hanus, Y. Ellinger, *J. Phys. Chem. A* **1997**, *101*, 299.
[26] A. T. Benjelloun, A. Daoudi, H. Chermette, *J. Chem. Phys.* **2004**, *121*, 7207.
[27] A. T. Benjelloun, A. Daoudi, H. Chermette, *Mol. Phys.* **2005**, *103*, 317.
[28] A. T. Benjelloun, A. Daoudi, H. Chermette, *J. Chem. Phys.* **2005**, *122*, 154304.
[29] C. Gourlaouen, J.-P. Piquemal, O. Parisel, *J. Chem. Phys.* **2006**, *124*, 174311.
[30] X. Wang, L. Andrews, *J. Am. Chem. Soc.* **2003** *125*, 6581.
[31] X. Wang, L. Andrews, G. V. Chertihin, P. F. Souter, *J. Phys. Chem. A* **2002**, *106*, 6302.
[32] It is worth noting that some data are available for poly-leaded structures: a) S. Varga, B. Fricke, H. Nakamatsu, T. Mukoyama, J. Anton, D. Geschke, A. Heitmann, E. Engel, T. Başuğ, *J. Chem. Phys.* **2000**, *112*, 3499; b) K. Balasubramanian, K. S. Pitzer, *J. Chem. Phys.* **1983**, *78*, 321; c) V. E. Bondibey, J. H. English, *J. Chem. Phys.* **1977**, *67*, 3405; d) A. Hoareau, P. Melinon, B. Cabaud, D. Rayne, B. Tribollet, M. Broyer, *Chem. Phys. Lett.* **1988**, *143*, 602; e) J. Ho, M. Polak, W. C. Lineberger, *J. Chem. Phys.* **1992**, *96*, 144.
[33] K. Balasubramanian, *J. Chem. Phys.* **1988**, *89*, 5731.
[34] P. Schwerdtfeger, H. Silberbach, B. Miehlich, *J. Chem. Phys.* **1989**, *90*, 762.
[35] S. G. Wang, W. H. E. Schwarz, *J. Mol. Struct. THEOCHEM* **1995**, *338*, 347.
[36] N. A. Richardson, J. C. Rienstra-Kiracofe, H. F. Schaefer III, *J. Am. Chem. Soc.* **1999**, *121*, 10813.
[37] N. Matsunaga, S. Koseki, M. S. Gordon, *J. Chem. Phys.* **1996**, *104*, 7988.
[38] H. Cox, A. J. Stace, *J. Am. Chem. Soc.* **2004**, *126*, 3939.
[39] J. Kapp, M. Remko, P. von Ragué Schleyer, *J. Am. Chem. Soc.* **1996**, *118*, 5745.
[40] A. Szabados, M. Hargittai, *J. Phys. Chem. A* **2003**, *107*, 4314.
[41] S. Escalante, R. Vargas, A. Vela, *J. Phys. Chem. A* **1999**, *103*, 5590.
[42] J.-P. Cornard, C. Lapouge, *Chem. Phys. Lett.* **2007**, *438*, 41.
[43] T. Enevoldsen, L. Visscher, T. Saue, H. J. Aagaard Jensen, J. Oddershede, *J. Chem. Phys.* **2000**, *112*, 3493.
[44] R. D. Hancock, J. H. Reibenspies, H. Maumela, *Inorg. Chem.* **2004**, *43*, 2981.
[45] C. Gourlaouen, O. Parisel, *Angew. Chem.* **2007**, *119*, 559; *Angew. Chem. Int. Ed.* **2007**, *46*, 553.
[46] C. Gourlaouen, PhD Thesis, Université Pierre et Marie Curie, Paris 6, Paris, **2006**.
[47] L. Zhang, J. Dong, M. Zhou, *J. Chem. Phys.* **2000**, *113*, 8700.
[48] R. J. Gillespie, R. S. Q. Nyholm, *Rev. Chem. Soc.* **1957**, *11*, 339.
[49] R. J. Gillespie, I. Hargittai, *The VSEPR model of molecular geometry*, Allyn and Bacon, Boston (MA, USA), **1991**.
[50] R. J. Gillespie, P. L. A. Popelier, *Chemical bonding and molecular geometry*, Oxford University Press, Oxford (UK), **2001**.
[51] a) J.-P. Piquemal, L. Perera, G. A. Cisneros, P. Ren, L. G. Pedersen, T. A. Darden, *J. Chem. Phys.* **2006**, *125*, 054511; b) J.-P. Piquemal, G. A. Cisneros, P. Reinhardt, N. Gresh, T. A. Darden, *J. Chem. Phys.* **2006**, *124*, 104101.
[52] Gaussian 03, Revision C.02, M. J. Frisch, G. W. Trucks, H. B. Schlegel, G. E. Scuseria, M. A. Robb, J. R. Cheeseman, J. A. Montgomery, Jr., T. Vreven, K. N. Kudin, J. C. Burant, J. M. Millam, S. S. Iyengar, J. Tomasi, V. Barone, B. Mennucci, M. Cossi, G. Scalmani, N. Rega, G. A. Petersson, H. Nakatsuji, M. Hada, M. Ehara, K. Toyota, R. Fukuda, J. Hasegawa, M. Ishida, T. Nakajima, Y. Honda, O. Kitao, H. Nakai, M. Klene, X. Li, J. E. Knox, H. P. Hratchian, J. B. Cross, V. Bakken, C. Adamo, J. Jaramillo, R. Gomperts, R. E. Stratmann, O. Yazyev, A. J. Austin, R. Cammi, C. Pomelli, J. W. Ochterski, P. Y. Ayala, K. Morokuma, G. A. Voth, P. Salvador, J. J. Dannenberg, V. G. Zakrzewski, S. Dapprich, A. D. Daniels, M. C. Strain, O. Farkas, D. K. Malick, A. D. Rabuck, K. Raghavachari, J. B. Foresman, J. V. Ortiz, Q. Cui, A. G. Baboul, S. Clifford, J. Cioslowski, B. B. Stefanov, G. Liu, A. Liashenko, P. Piskorz, I. Komaromi, R. L. Martin, D. J. Fox, T. Keith, M. A. Al-Laham, C. Y. Peng, A. Nanayakkara, M. Challacombe, P. M. W. Gill, B. Johnson, W. Chen, M. W. Wong, C. Gonzalez, J. A. Pople, Gaussian, Inc., Wallingford CT, **2004**.
[53] C. Lee, W. Yang, R. G. Par, *Phys. Rev. B* **1988**, *37*, 785.
[54] A. D. Becke, *J. Chem. Phys.* **1993**, *98*, 5648.
[55] C. Gourlaouen, J.-P. Piquemal, T. Saue, O. Parisel, *J. Comput. Chem.* **2006**, *27*, 142.
[56] For a recent review, see, for example: M. Dolg, in: *Modern Methods and Algorithms of Quantum Chemistry*, edited by J. Grotendorst, John von Neumann Institute for Computing, Jülich (Germany), **2000**; or: H. Stoll, B. Metz, M. Dolg, *J. Comput. Chem.* **2002**, *23*, 767.
[57] P. J. Hay, W. R. Wadt, *J. Chem. Phys.* **1985**, *82*, 270, P. J. Hay, W. R. Wadt, *J. Chem. Phys.* **1985**, *82*, 284 and P. J. Hay, W. R. Wadt, *J. Chem. Phys.* **1985**, *82*, 299.
[58] W. Kuelche, M. Dolg, H. Stoll, H. Preuss, *Mol. Phys.* **1991**, *74*, 1245.
[59] R. B. Ross, J. M. Powers, T. Atashroo, W. C. Ermler, L. A. LaJohn, P. A. Christiansen, *J. Chem. Phys.* **1990**, *93*, 6654.
[60] This basis set was obtained from the Extensible Computational Chemistry Environment Basis Set Database, Version 02/25/04, as developed and distributed by the Molecular Science Computing Facility, ***E**nvironmental and **M**olecular **S**ciences **L**aboratory* which is part of the Pacific Northwest Laboratory, P. O. Box 999, Richland, Washington 99352, USA, and funded by the US Department of Energy. The Pacific Northwest Laboratory is a multi-program laboratory operated by Battelle Memorial Institute for the US Department of Energy under contract DE-AC06-76RLO 1830. See URL: http://www.emsl.pnl.gov/forms/basisform.html
[61] K. A. Peterson, *J. Chem. Phys.* **2003**, *119*, 11099.
[62] T. H. Dunning Jr. , *J. Chem. Phys.* **1989**, *90*, 1007.
[63] K. Faegri, *Theor. Chem. Acc.* **2001**, *105*, 252.
[64] *Dirac, a relativistic ab initio electronic structure program*, Release DIRAC04 (2004), written by H. J. Aa. Jensen, T. Saue, and L. Visscher with contributions from V. Bakken, E. Eliav, T. Enevoldsen, T. Fleig, O. Fossgaard, T. Helgaker, J. Laerdahl, C. V. Larsen, P. Norman, J. Olsen, M. Pernpointner, J. K. Pedersen, K. Ruud, P. Salek, J. N. P. van Stralen, J. Thyssen, O. Visser, T. Winther. See URL: http://dirac.chem.sdu.dk
[65] T. Saue, T. Helgaker, *J. Comput. Chem.* **2002**, *23*, 814.
[66] O. Fossgaard, O. Gropen, M. Corral Valero, T. Saue, *J. Chem. Phys.* **2003**, *118*, 10418.
[67] L. Visscher, T. Saue, *J. Chem. Phys.* **2000**, *113*, 3996.
[68] L. Visscher, K. G. Dyall, *At. Data Nucl. Data Tables* **1997**, *67*, 207.
[69] S. F. Boys, F. Bernardi, *Mol. Phys.* **1970**, *19*, 553.
[70] P. Hobza, R. Zahradník, *Chem. Rev.* **1988**, *88*, 871.
[71] K. Clemenger, *Phys. Rev. B* **1985**, *32*, 1359.
[72] C. Yannouleas, U. Landman, *Phys. Rev. B* **1996**, *54*, 7690.

[73] J. Zhao, Y. Luo, G. Wang, *Eur. Phys. J. D* **2001**, *14*, 309.
[74] W. A. de Heer, *Rev. Mod. Phys.* **1993**, *65*, 611.
[75] S. K. Nayak, P. Jena, V. S. Stepanyuk, W. Hergert, K. Wildberger, *Phys. Rev. B* **1997**, *56*, 6952.
[76] J. Wang, G. Wang, J. Zhao, *Phys. Rev. B* **2001**, *64*, 205411.
[77] G. Pascoli, H. Lavendy, *Eur. Phys. J. D* **2002**, *19*, 339.
[78] V. Kumar, *Eur. Phys. J. D* **2003**, *24*, 227.
[79] V. Kumar, Y. Kawazoe, *Phys. Rev. B* **2002**, *65*, 073404.
[80] L. Ma, J. Zhao, J. Wang, Q. Lu, L. Zhu, G. Wang, *Chem. Phys. Lett.* **2005**, *411*, 279.
[81] L.-G. Guo, G.-F. Zhao, Y.-H. Luo, *J. Chem. Phys.* **2007**, *126*, 234704.
[82] a) J. E. Carpenter, PhD thesis, University of Wisconsin, Madison, WI, **1987**; b) A. E. Reed, L. A. Curtiss, F. Weinhold, *Chem. Rev.* **1988**, *88*, 899; c) NBO Version 3.1, E. D. Glendening, A. E. Reed, J. E. Carpenter, F. Weinhold.
[83] A. D. Becke, K. E. Edgecombe, *J. Chem. Phys.* **1990**, *92*, 5397.
[84] A. Savin, R. Nesper, S. Wengert, T. F. Fässler, *Angew. Chem.* **1997**, *109*, 1892; *Angew. Chem. Int. Ed. Engl.* **1997**, *36*, 1808 and .
[85] S. Noury, X. Krokidis, F. Fuster, B. Silvi, TopMod Package, **1997**. This package is available on the web site of the Laboratoire de Chimie Théorique, Université Pierre et Marie Curie (UMR 7616, CNRS-UPMC), URL: www.lct.jussieu.fr (see the personal homepage of Prof. B. Silvi).
[86] S. Noury, X. Krokidis, F. Fuster, B. Silvi, *Comput. Chem. Eng.* **1999**, *23*, 597.
[87] B. Silvi, A. Savin, *Nature* **1994**, *371*, 683.
[88] A. Savin, B. Silvi, F. Colonna, *Can. J. Chem.* **1996**, *74*, 1088.
[89] For a recent review: J. Poater, M. Duran, M. Solà, B. Silvi, *Chem. Rev.* **2005**, *105*, 3911.
[90] A. Savin, *J. Chem. Sci.* **2005**, *117*, 473.
[91] M. Kohout, A. Savin, *J. Comput. Chem.* **1997**, *18*, 2000.
[92] L. Joubert, B. Silvi, G. Picard, *Theor. Chem. Acc.* **2000**, *104*, 109.
[93] P. S. Bagus, K. Hermann, C. W. Bauschlicher Jr. , *J. Chem. Phys.* **1984**, *80*, 4378.
[94] P. S. Bagus, K. Hermann, C. W. Bauschlicher Jr. , *J. Chem. Phys.* **1984**, *81*, 1966.
[95] P. S. Bagus, F. Illas, *J. Chem. Phys.* **1992**, *96*, 8962.
[96] W. J. Stevens, W. H. Fink, *Chem. Phys. Lett.* **1987**, *139*, 15.
[97] K. Morokuma, *Acc. Chem. Res.* **1977**, *10*, 294.
[98] K. Kitaura, K. Morokuma, *Int. J. Quantum Chem.* **1976**, *10*, 325.
[99] J.-P. Piquemal, R. Chelli, P. Procacci, N. Gresh, *J. Phys. Chem. A* **2007**, *111*, 8170.
[100] G. te Velde, M. Bickelhaupt, E. J. Baerends, S. J. A. Van Gisbergen, C. Fonseca Guerra, J. G. Snijders, T. Ziegler, *J. Comput. Chem.* **2001**, *22*, 1.
[101] F. M. Bickelhaupt, E. J. Baerends, *Rev. Comput. Chem.* **2000**, *15*, 1.
[102] T. Ziegler, A. Rauk, *Inorg. Chem.* **1979**, *18*, 1755.
[103] M. Dupuis, A. Marquez and E. R. Davidson, "HONDO95.3", Quantum Chemistry Program Exchange (QCPE) Indiana University, Bloomington, IN 47405.
[104] J.-P. Piquemal, A. Marquez, O. Parisel, C. Giessner-Prettre, *J. Comput. Chem.* **2005**, *26*, 1052.
[105] K. Morokuma, *J. Chem. Phys.* **1971**, *55*, 1236.
[106] K. Kitaura, K. Morokuma, *Int. J. Quantum Chem.* **1976**, *10*, 325.
[107] M. S. Gordon, J. H. Jensen in: *Encyclopaedia of Computational Chemistry, Vol. V* (Ed.: P. von Ragué Schleyer), Wiley, Chichester, **1998**, pp. 3198–3214.
[108] W. J. Stevens, W. Fink, *Chem. Phys. Lett.* **1987**, *139*, 15.
[109] M. Neyman, S. Ph. Ruzankin, N. Rösch, *Chem. Phys. Lett.* **1995**, *246*, 546.
[110] S. C. Chung, S. Kruger, S. Ph. Ruzankin, G. Pacchioni, N. Rösch, *Chem. Phys. Lett.* **1996**, *248*, 109.
[111] A. M. Márquez, N. López, M. García-Hernández, F. Illas, *Surf. Sci.* **1999**, *442*, 463.
[112] A. Ricca, C. W. Bauschlicher, *J. Phys. Chem. A* **2002**, *106*, 3219.
[113] A. J. Lupinetti, S. Fau, G. Frenking, S. H. Strauss, *J. Phys. Chem. A* **1997**, *101*, 9551.
[114] a) P. K. Hurlburt, J. J. Rack, J. S. Luck, S. F. Dec, J. D. Webb, O. P. Anderson, S. H. Strauss, *J. Am. Chem. Soc.* **1994**, *116*, 10003; b) J. J. Rack, J. D. Webb, S. H. Strauss, *Inorg. Chem.* **1996**, *35*, 277; c) P. K. Hurlburt, O. P. Anderson, S. H. Strauss, *J. Am. Chem. Soc.* **1991**, *113*, 6277.
[115] C. Bach, H. Willner, C. Wang, S. J. Rettig, J. Trotter, F. Aubke, *Angew. Chem.* **1996**, *108*, 2104; *Angew. Chem. Int. Ed. Engl.* **1996**, *35*, 1974.
[116] G. Frenking, N. Fröhlich, *Chem. Rev.* **2000**, *100*, 717.
[117] G. Frenking, C. Loschen, A. Krapp, S. Fau, S. H. Strauss, *J. Comput. Chem.* **2007**, *28*, 117.
[118] R. K. Hocking, T. W. Hambley, *Organometallics* **2007**, *26*, 2815.
[119] A. M. Badger, *J. Chem. Phys.* **1935**, *3*, 710.
[120] A. Bérces, T. Ziegler, *J. Phys. Chem.* **1994**, *98*, 12233.
[121] A. Bérces, T. Ziegler, *J. Phys. Chem.* **1995**, *99*, 11417.
[122] A. de la Lande, H. Gérard, V. Moliner, G. Izzet, O. Reinaud, O. Parisel, *J. Biol. Inorg. Chem.* **2006**, *11*, 593.
[123] A. de la Lande, V. Moliner, O. Parisel, *J. Chem. Phys.* **2007**, *126*, 035102.
[124] J. Pilmé, E. A. Robinson, R. J. Gillespie, *Inorg. Chem.* **2006**, *45*, 6198.
[125] A. R. Mahjoub, X. Zhang, K. Seppelt, *Chem. Eur. J.* **1995**, *1*, 261.
[126] E. A. Robinson, R. J. Gillespie, *Inorg. Chem.* **2003**, *42*, 3865.
[127] R. J. Gillespie, E. A. Robinson, *Chem. Soc. Rev.* **2005**, *34*, 396.
[128] E. A. Robinson, G. L. Heard, R. J. Gillespie, *J. Mol. Struct.* **1999**, *485–486*, 305.
[129] H. Gérard, A. de la Lande, J. Maddaluno, O. Parisel, M. E. Tuckerman, *J. Phys. Chem. A* **2006**, *110*, 4787.
[130] K. O. Christe, W. W. Wilson, G. W. Drake, D. A. Dixon, J. A. Boatz, R. Z. Gnann, *J. Am. Chem. Soc.* **1998**, *120*, 4711.
[131] K. O. Christe, E. C. Curtis, D. A. Dixon, H. P. Mercier, J. C. P. Sanders, G. J. Schrobilgen, *J. Am. Chem. Soc.* **1991**, *113*, 3351.
[132] K. O. Christe, W. W. Wilson, R. V. Chirakal, J. C. P. Sanders, G. J. Schrobilgen, *Inorg. Chem.* **1990**, *29*, 3506.
[133] M. Kaupp, Ch. Van Wüllen, R. Franke, F. Schmitz, W. Kutzelnigg, *J. Am. Chem. Soc.* **1996**, *118*, 11939.
[134] D. J. Payne, R. G. Egdell, A. Walsh, G. W. Watson, J. Guo, P.-A. Glans, T. Learmonth, K. E. Smith, *Phys. Rev. Lett.* **2006**, *96*, 157403.
[135] A. Walsh, G. W. Watson, *J. Phys. Chem. B* **2005**, *109*, 18868.
[136] A. R. Boate, J. R. Morton, K. F. Preston, *J. Phys. Chem.* **1978**, *82*, 718.

Received: August 14, 2007
Published online: January 29, 2008

